

STRUCTURAL AND SURFACE PROPERTIES OF ZINC-TELLURITE
GLASS DOPED WITH SILICON DIOXIDE

SYARINIE BINTI AZMI

UNIVERSITI TEKNOLOGI MALAYSIA

STRUCTURAL AND SURFACE PROPERTIES OF ZINC–TELLURITE GLASS
DOPED WITH SILICON DIOXIDE

SYARINIE BINTI AZMI

A thesis submitted in fulfilment of the
requirements for the award of the degree of
Master of Philosophy

Faculty of Science
Universiti Teknologi Malaysia

MARCH 2018

*To my beloved mother, step father, siblings, grandma, aunts, uncles, cousins, late
father who was very proud of me and other family members*

ACKNOWLEDGEMENT

Alhamdulillah, first and foremost, all praise to Allah SWT, the Almighty, for giving me the strength, courage and patience to finish this study. It is a great pleasure to acknowledge my deepest thanks and gratitude to my main project supervisor, Associate Professor Dr. Ramli Arifin for encouragement, guidance, advice, motivation and his kind supervision. I am also very thankful to my co-supervisor Associate Professor Dr. Sib Krishna Ghoshal for his advice, guidance and critics throughout completing this study.

I also take this opportunity to record my sincere thanks to all Advance Optical Material Research Group members for their help and encouragement. My sincere appreciation to all staffs members Faculty of Science, Universiti Teknologi Malaysia for their help and assistance. Financial supports of MoHE through Vot. GUP/RU/UTM 4F650, 18H68, 17H19, 13H50 and 12H42 are appreciated. My fellow postgraduate students and friends are also acknowledged for their moral support. Not to forget, I am really grateful to all my family members for their endless love and support throughout this journey.

I also place on record, my sense of gratitude to one and all who, directly or indirectly, have lent their helping hand in this venture. Last but not least, I would like to acknowledge the Ministry of Education, Malaysia for their financial support.

ABSTRACT

This thesis studied the influence of silicon dioxide (SiO_2) on the physical, thermal, structural and surface properties of zinc-tellurite glass. A series of transparent ternary tellurite glass systems with composition $(80-x)\text{TeO}_2-20\text{ZnO}-x\text{SiO}_2$, where $x = 0$ till 0.20 mol% were synthesized via conventional melt-quenching method. The effects of varying SiO_2 contents on the glass density, structural characteristics, thermal properties, water contact angle (WCA), surface roughness and surface morphology were investigated. The amorphous nature of the glass was confirmed using X-ray diffraction measurement. The increase in the SiO_2 contents reduced the density from 5.55 to 5.53 $\text{g}\cdot\text{cm}^{-3}$ and enhanced the molar volume from 25.96 to 26.06 $\text{cm}^3\cdot\text{mol}^{-1}$. Differential thermal analysis revealed the increase of glass transition temperature (T_g) with the increase of SiO_2 contents. The thermal stability factor was found to vary between 79.9 to 81.5°C depending on the glass composition. Glass morphologies were characterized using atomic force microscopy and WCA measurements. Glass surface roughness as much as 10 nm was attained which is higher than normal glass. The optimal value for WCA was discerned to be 101° and the minimum surface energy was found to be 0.06 $\text{N}\cdot\text{m}^{-1}$ for glass sample with 0.1 mol% of SiO_2 indicating a glass with low wettability compared to other zinc-tellurite glass. The structural characteristics of glass samples were investigated using Fourier transform infrared (FTIR) spectroscopy in the range of 600 – 4000 cm^{-1} . The FTIR results showed the tellurium atom coordination changes from TeO_4 to TeO_3 with the increase of SiO_2 contents. For TeO_4 coordination, the infrared band peaks occurred between 642.8 and 661.7 cm^{-1} whereas for TeO_3 , the peaks were observed between 784.7 and 773.1 cm^{-1} . Field emission scanning electron microscopy and energy dispersive X-ray spectroscopy were performed on the glass sample. The surface morphology of glass system appeared rougher with the addition of SiO_2 content up to 0.1 mol% which is better compared to normal glass. Overall, the physical, thermal and structural properties of the proposed zinc-tellurite glass system were marginally changed while the surface properties were significantly improved with the inclusion of SiO_2 .

ABSTRAK

Tesis ini mengkaji tentang pengaruh silikon dioksida (SiO_2) terhadap sifat fizikal, terma, struktur dan permukaan kaca zink-tellurit. Satu siri sistem kaca tellurit ternari lutsinar dengan komposisi $(80-x)\text{TeO}_2-20\text{ZnO}-x\text{SiO}_2$, dengan $x = 0$ hingga 0.20 mol% telah disintesis melalui kaedah pelindapan peleburan konvensional. Kesan perubahan kandungan SiO_2 terhadap ketumpatan kaca, ciri struktur, sifat terma, sudut sentuh air (WCA), kekasaran permukaan dan morfologi permukaan telah dikaji. Sifat amorfus kaca telah disah menggunakan pengukuran pembelauan sinar-X. Peningkatan kandungan SiO_2 telah mengurangkan ketumpatan daripada 5.55 kepada 5.53 $\text{g}\cdot\text{cm}^{-3}$ dan meningkatkan isipadu molar daripada 25.96 kepada 26.06 $\text{cm}^3\cdot\text{mol}^{-1}$. Analisis terma pembeza mendedahkan peningkatan suhu peralihan kaca (T_g) dengan peningkatan kandungan SiO_2 . Faktor kestabilan terma didapati berubah antara 79.9 kepada 81.5°C bergantung kepada komposisi kaca. Morfologi sampel kaca telah diciri menggunakan mikroskopi daya atom dan pengukuran WCA. Kekasaran permukaan kaca sebanyak 10 nm telah dicapai iaitu lebih tinggi berbanding kaca biasa. Nilai optimum WCA yang telah diperolehi ialah 101° dan tenaga permukaan minimum yang didapati ialah 0.06 $\text{N}\cdot\text{m}^{-1}$ bagi sampel kaca dengan 0.1 mol% SiO_2 menggambarkan kaca dengan kebolehbasahan yang rendah berbanding kaca zink-tellurit yang lain. Ciri struktur sampel kaca telah dikaji menggunakan spektroskopi inframerah transformasi Fourier (FTIR) dalam julat 600 – 4000 cm^{-1} . Keputusan FTIR menunjukkan koordinasi atom tellurium berubah daripada TeO_4 kepada TeO_3 dengan pertambahan kandungan SiO_2 . Bagi koordinasi TeO_4 , puncak jalur inframerah terjadi antara 642.8 dan 661.7 cm^{-1} sedangkan bagi TeO_3 pula, puncaknya telah dicerap antara 784.7 dan 773.1 cm^{-1} . Mikroskopi elektron pengimbasan pelepasan medan dan spektroskopi sinar-X tenaga tersebar telah dilaksanakan terhadap sampel kaca tersebut. Morfologi permukaan sistem kaca kelihatan lebih kasar dengan penambahan kandungan SiO_2 sehingga 0.1 mol% iaitu lebih baik berbanding kaca biasa. Secara keseluruhannya, sifat fizikal, terma dan struktur sistem kaca zink tellurit yang dicadangkan telah mengalami perubahan secara marginal manakala sifat permukaan telah bertambahbaik secara signifikan dengan penambahan SiO_2 .

TABLE OF CONTENTS

CHAPTER	TITLE	PAGE
	DECLARATION	ii
	DEDICATION	iii
	ACKNOWLEDGEMENT	iv
	ABSTRACT	v
	ABSTRAK	vi
	TABLE OF CONTENTS	vii
	LIST OF TABLES	x
	LIST OF FIGURES	xii
	LIST OF SYMBOLS	xvii
	LIST OF ABBREVIATIONS	xviii
	LIST OF APPENDICES	xix
1	INTRODUCTION	1
	1.1 Introduction	1
	1.2 Background of the Study	1
	1.3 Problem Statement	3
	1.4 Objectives of the Study	4
	1.5 Scope of the Study	4
	1.6 Significance of the Study	5

2	LITERATURE REVIEW	6
2.1	Introduction	6
2.2	Structure of Tellurite	6
2.3	Effect of ZnO to Structure of Tellurite	9
2.4	Influence of SiO ₂ to Matrix System	10
2.5	Physical Properties	12
2.6	X-Ray Diffraction Studies	15
2.7	Structural Studies	19
2.8	Thermal Studies	23
2.9	Atomic Force Microscopy Imaging	27
2.10	Surface Morphology Studies	28
2.11	Water Contact Angle and Surface Tension Studies	30
3	METHODOLOGY	37
3.1	Introduction	37
3.2	Glass Preparation	38
3.3	X-Ray Diffraction Measurement	41
3.4	Fourier Transform Infrared Spectroscopy	42
3.5	Differential Thermal Analyzer	43
3.6	Field Emission Scanning Electron Microscopy and Energy Dispersive X-ray Spectroscopy	44
3.7	Atomic Force Microscopy	47
3.8	Contact Angle Measurement and Calculation of Surface Tension	48
4	RESULTS AND DISCUSSION	50
4.1	Introduction	50
4.2	Physical Properties	51
4.3	Density Analysis	52
4.4	Amorphous Phase Analysis	54

4.5	Structure Analysis	55
4.6	Thermal Analysis	58
4.7	Surface Morphologies and Element Composition Analysis	62
4.8	Topography Analysis	66
4.9	Water Contact Angle (WCA) Analysis	72
4.10	Relationship between WCA and Surface Tension	75
5	CONCLUSION	78
5.1	Introduction	78
5.2	Conclusion	78
5.3	Future Works	80
	REFERENCES	82
	APPENDICES	92

LIST OF TABLES

TABLE NO.	TITLE	PAGE
Table 2.1	The glass density and molar volume of zinc-tellurite glass system	14
Table 2.2	IR absorption band assignment (cm^{-1}) for various glass system	23
Table 2.3	Previous study of thermal analysis	26
Table 2.4	Surface tension data of various liquid	32
Table 3.1	The nominal composition of $(80-x)\text{TeO}_2-20\text{ZnO}-(x)\text{SiO}_2$ glass system	41
Table 4.1	The nominal composition and physical appearance of $(80-x)\text{TeO}_2-20\text{ZnO}-(x)\text{SiO}_2$ glass system	51
Table 4.2	Density and molar volume of $(80-x)\text{TeO}_2-20\text{ZnO}-(x)\text{SiO}_2$ glass system	52

Table 4.3	Assignments of the IR absorption band (cm^{-1}) in glass samples	56
Table 4.4	IR absorption band (cm^{-1}) of $(80-x)\text{TeO}_2-20\text{ZnO}-(x)\text{SiO}_2$ glass	57
Table 4.5	The thermal parameters (T_g), (T_c) and (T_m) ($^\circ\text{C}$) of synthesized glasses, errors in temperature measurement is ($\pm 0.1^\circ\text{C}$)	61
Table 4.6	Comparison for actual and nominal element compositions for sample with and without addition of SiO_2	65
Table 4.7	Roughness parameters (R_a , R_z , R_p , RMS) with different SiO_2 concentration of glass samples	70
Table 4.8	Surface roughness and water contact angle (WCA) of synthesized glasses	71
Table 4.9	WCA values of the prepared glass	74
Table 4.10	WCA and Surface Tension value of the prepared glass	76

LIST OF FIGURES

FIGURE NO.	TITLE	PAGE
Figure 2.1	Structure of TeO_{3+1} and TeO_3	8
Figure 2.2	Basic chains of zinc-tellurite system	10
Figure 2.3	Basic structure of silicon dioxide	11
Figure 2.4	Illustration of Bragg reflection from a set of parallel planes	16
Figure 2.5	XRD patterns of the glass electrolytes containing various Li_2O concentrations of $(85-x)\text{TeO}_2-x\text{Li}_2\text{O}-15\text{ZnO}$ where $x=0,5,10$ and 15 mol%	17
Figure 2.6	The XRD pattern of zinc-tellurite and pure tellurite glass for $(\text{ZnO})_x(\text{TeO}_2)_{1-x}$ (where $x=0$ to 0.4 mol%)	18
Figure 2.7	Typical XRD pattern of Sm^{3+} doped zinc-tellurite glass	18

Figure 2.8	Modes of stretching and bending	20
Figure 2.9	Illustrations of normal modes of vibration (cm^{-1})	21
Figure 2.10	FTIR spectra of $(\text{TeO}_2)_{1-x}(\text{ZnO})_x$ glasses with various composition	22
Figure 2.11	FTIR spectra of Sm^{3+} doped zinc-tellurite glass sample with band assignments	22
Figure 2.12	A typical DTA curves of the tellurite glasses	25
Figure 2.13	DTA curves for zinc-tellurite glass sample	25
Figure 2.14	DTA curve of Sm^{3+} doped zinc-tellurite glass	26
Figure 2.15	3D topography and roughness profile of glazed surface of the lithium disilicate glass ceramic	28
Figure 2.16	The example of (a) FESEM image and (b) EDX spectra of $70\text{TeO}_2 + 20\text{ZnO} + 10\text{Na}_2\text{O} + 1\text{Er}_2\text{O}_3 + 0.6 \text{ Au}$ glass system to verify the element present in glass matrix	30
Figure 2.17	Illustration of contact angle formed by sessile liquid drops on a smooth homogeneous solid surface	31
Figure 2.18	Surface tension caused by unbalanced forces of liquid molecules at the surface	31

Figure 2.19	The three phenomenon for surface energy, wetting behavior and surface roughness on the hydrophobicity of solid surface	36
Figure 3.1	The cooling schedule of prepared glass sample	39
Figure 3.2	Flow chart of sample preparation	40
Figure 3.3	Schematic diagram of X-ray diffractometer	42
Figure 3.4	Schematic diagram of Differential Thermal Analyzer	44
Figure 3.5	Schematic diagram of Field Emission Scanning Electron Microscopy	46
Figure 3.6	Block diagram of Energy Dispersive X-ray detector	47
Figure 3.7	Block diagram of AFM working	48
Figure 4.1	Glass samples of $(80-x)\text{TeO}_2-20\text{ZnO}-x\text{SiO}_2$ where $x = 0.00, 0.05, 0.10, 0.15$ and 0.20 mol%	51
Figure 4.2	SiO_2 content dependent variation of glass density	53
Figure 4.3	SiO_2 content dependent variation of glasses molar volume	54
Figure 4.4	XRD pattern of $79.90\text{TeO}_2-20\text{ZnO}-0.1\text{SiO}_2$ glass sample	55

Figure 4.5	Infrared transmission spectra for $(80-x)\text{TeO}_2 - 20\text{ZnO} - (x)\text{SiO}_2$ glass system	56
Figure 4.6	DTA curves of synthesized glass system indicating (T_g) , (T_c) and (T_m) Exo : Exothermic (upward) and Endo : Endothermic (downward)	60
Figure 4.7	Variation of T_g , T_c and T_m with SiO_2 contents	61
Figure 4.8	Variation of glass thermal stability with SiO_2 content	62
Figure 4.9	FESEM images of glass sample (a) without SiO_2 (S1) and (b) with addition of SiO_2 (S3)	63
Figure 4.10	The EDX spectrum of glass sample (a) without SiO_2 (S1) and (b) with addition of SiO_2 (S3)	65
Figure 4.11	AFM image of (a) 3D topography, (b) 2D surface and (c) surface roughness profile of glass sample at concentration of 0.00 mol% SiO_2 (S1)	67
Figure 4.12	AFM image of (a) 3D topography, (b) 2D surface and (c) surface roughness profile of glass sample at concentration of 0.05 mol% SiO_2 (S2)	67
Figure 4.13	AFM image of (a) 3D topography, (b) 2D surface and (c) surface roughness profile of	68

	glass sample at concentration of 0.10 mol% SiO ₂ (S3)	
Figure 4.14	AFM image of (a) 3D topography, (b) 2D surface and (c) surface roughness profile of glass sample at concentration of 0.15 mol% SiO ₂ (S4)	69
Figure 4.15	AFM image of (a) 3D topography, (b) 2D surface and (c) surface roughness profile of glass sample at concentration of 0.20 mol% SiO ₂ (S5)	69
Figure 4.16	SiO ₂ content dependent of the surface roughness and WCA	72
Figure 4.17	Water contact angle for water drop at glass surfaces containing SiO ₂ of (a) 0.00 mol% (S1), (b) 0.05 mol% (S2), (c) 0.10 mol% (S3), (d) 0.15 mol% (S4) and (e) 0.20 mol% (S5)	73
Figure 4.18	Water contact angle dependent on SiO ₂ content	75
Figure 4.19	Relationship between WCA and Surface Tension	76

LIST OF SYMBOLS

n	-	Refractive index
n	-	Moles
P	-	Pressure
ρ	-	Density
r	-	Roughness of the surface
RMS	-	Root mean square roughness
R_a	-	Average roughness
R_p	-	Maximum peak
R_z	-	Mean height of roughness in 10 points
T	-	Temperature
T_m	-	Melting temperature
T_g	-	Glass transition temperature
T_c	-	Crystalline temperature
θ	-	Water contact angle
λ	-	Wavelength
γ_{lv}	-	Interfacial tension between liquid and vapour
γ_{sv}	-	Interfacial tension between solid and vapour
γ_{sl}	-	Interfacial tension between solid and liquid
δA	-	Total surface area
δG	-	Total surface free energy
θ_w	-	Wenzel's contact angle
θ_Y	-	Young's contact angle

LIST OF ABBREVIATIONS

AFM	-	Atomic Force Microscopy
BO	-	Bridging Oxygen
EDX	-	Energy Dispersive X-ray
FESEM	-	Field Emission Scanning Electron Microscopy
FTIR	-	Fourier Transform Infrared
IR	-	Infrared
NBO	-	Non-bridging Oxygen
NPs	-	Nanoparticles
RMS	-	Root Mean Square
Tbp	-	Trigonal Bipyramid
Tp	-	Trigonal Pyramid
WCA		Water Contact Angle
XRD	-	X-ray Diffraction

LIST OF APPENDICES

TITLE	PAGE
APPENDIX A	
Figure A.1 : Density meter by Mettler Toledo available at Department of Physics, Faculty of Science, UTM	92
Figure A.2 : Rigaku SmartLab X-ray diffractometer available at University Industry Research Laboratory, UTM	93
Figure A.3 : Perkin Elmer FTIR Spectrometer Frontier GPOB available at Department of Chemistry, Faculty of Science, UTM	93
Figure A.4 : Perkin Elmer STA 8000 University Industry Research Laboratory, UTM	94
Figure A.5 : The Hitachi SU8020 FESEM with EDX analysis available at University Industry Research Laboratory, UTM	94
Figure A.6 : Atomic Force Microscope at	95

Department of Physics, Faculty of
Science, UTM

Figure A.7: Optical Contact Angle meter of Data	95
Physics available in Advance	
Membrane Technology Research	
Centre (AMTEC), UTM.	

APPENDIX B

Calculation of Batch Sample Composition	96
---	----

APPENDIX C

Calculation for Density of Sample	98
-----------------------------------	----

Calculation for Uncertainty of Density	99
--	----

Calculation for Molar Volume of Sample	100
--	-----

Calculation for Uncertainty of Molar Volume	100
---	-----

APPENDIX D

Calculation of Surface Tension	102
--------------------------------	-----

APPENDIX E

FTIR Spectra	103
--------------	-----

APPENDIX F

List of Publications	105
----------------------	-----

CHAPTER 1

INTRODUCTION

1.1 Introduction

In this chapter, the general information about this study will be provided in details. This study is about hydrophobic effect on tellurite glass with variation of dopant and modifier. The research background, problem statement, objective of the study, scope of study, significance of study and outline of study will be described in this chapter.

1.2 Background of the Study

In general, glass is a versatile and sometimes very enigmatic substance. It can be made stronger than steel or soluble in water, a detector of nuclear radiations or the

source of a powerful laser beam depending upon composition (Pye, 1972). Glass is an amorphous solid or non-crystalline solids in which the atoms and molecules are not organized in periodic lattice pattern. The atomic arrangement of amorphous solids is no long range order but short or medium range order. In contrast, atomic arrangement in crystalline solids exhibit a property called long range order or translational periodicity which is the positions repeat in space in a regular array. The amorphous can be formed by fast cooling from a melt in order to avoid crystallization.

Tellurium oxide (TeO_2) based glasses has been scientific and technological interest due to their unique properties such as chemical durability, electrical conductivity, transmission capability, high dielectric constant, high refractive indices and low melting points (Nasu *et al.*, 1990; Tanaba *et al.*, 1990). Stanworth, (1952) and Burger *et al.*, (1985) stated that the application of tellurite glasses in industries such as electric, optical, electronic and other fields are immense due to their good semiconducting properties. Recently, tellurite glasses have gained wide attention because of their potential as hosts of rare earth elements for the development of fibres and lasers covering all the main telecommunication bands (Conti *et al.*, 2004), and promising materials for optical switching devices (Sidkey and Gaafar, 2004).

Besides that, tellurite glasses doped with heavy metal oxides or rare earth oxides (El-Mallawany *et al.*, 1995; El-Mallawany, 1998; Berthereau *et al.*, 1996) such as Nb_2O_3 , CeO_2 or ZnO recently have received great scientific interest because these oxides can change the optical and physical properties of the tellurite glasses. Furthermore, $\text{ZnO}-\text{TeO}_2$ system is another basic system that has good glass forming ability and used by many researchers. Sidebottom *et al.*, (1997) has reported that Zinc-tellurite glasses to be a suitable host for optically active rare earth ions because of the wide glass-formation range which is close to the extremum for binary tellurite glasses. In addition, $\text{ZnO}-\text{TeO}_2$ system was used as a basis for multicomponent optical glass synthesis and has been reported as a useful medium for ultralow loss (1 dB 1000 m⁻¹) optical fibers for wavelengths in the 3.5–4 μm region (Van Uitert and Wemple, 1978).

Therefore, from the coverage above it seems clear that tellurite glasses are strategically important solid materials. However, to my knowledge, using SiO_2 as one of the dopant in zinc-tellurite system is never been explored and documented. The hypersensitive transition of silicon ions manifest as anomalous sensitivity of line strength to the character of the dopant environment. Apart from their applications, there is a lack of data on structural investigation as well as the thermal properties of the zinc-tellurite glass system especially with addition of SiO_2 in the literature. Therefore, the aim of this research is to study the influence of SiO_2 on structural, thermal and surface texture properties of Zinc-tellurite glass system in order to understand the fundamental origin of such properties.

1.3 Problem Statement

The combination of tellurium oxide and zinc oxide forms stable glass system (Kozhukharov *et al.*, 1986). Zinc-tellurite glass system is widely used in lasers, lens, optical and solar applications including solar power plants and solar collectors. The intensity of the incident sunlight determines the power of conversion of solar light to electricity or water heating. However, the glass material used results in reflection losses though convection and radiation losses are minimized. One of the important properties in self-cleaning glasses is refractive index (n). In order to make the surfaces anti-reflective for solar cover glasses, a low refractive index such as SiO_2 which $n \leq 1.4$ is needed (Surekha and Sudararajan, 2015).

In addition, SiO_2 doped zinc-tellurite glass are expectedly last longer than silica thin films since the substrate do not need to recoating after a long period of time because of few factors such as air, water and sunlight. Other than that, the light can passed through the glass easily compared to silicate thin films since the light can

REFERENCES

- Asthana, R. and Sobzack, N. (2000). Wettability, Spreading and Interfacial Phenomena in High- Temperature Coatings. *Journal of Material Engineering*, 52 (1), 1-19.
- Awang, A., Ghoshal, S. K., Sahar, M. R., Arifin, R., and Nawaz, F. (2014). Non-Spherical Gold Nanoparticles Mediated Surface Plasmon Resonance in Er³⁺ Doped Zinc-Sodium Tellurite Glasses: Role of Heat Treatment. *Journal of Luminescence*, 149, 138-143.
- Ayuni, J. N., Halimah, M. K., Talib, Z. A., Sidek, H. A. A., Daud, W. M., Zaidan, A. W. and Khamirul, A. M. (2011). Optical Properties of Ternary TeO₂-B₂O₃-ZnO Glass System. *IOP Conference Series: Materials Science and Engineering*, 17, 1-8.
- Basu, B. J., Hariprakash, V., Aruna, S. T., Lakshmi, R. V., Manasa, J., and Shruthi, B. S. (2010). Effect of Microstructure and Surface Roughness on the Wettability of Superhydrophobic Sol-Gel Nanocomposite Coatings. *Journal of Sol-Gel Science and Technology*, 56, 278-286.
- Berthereau, A., Fargin, E., Villezusanne, A., Olazcuaga, R., Flem, G. L., and Ducasse, L. (1996). *Journal of Solid State Chemistry*, 126, 143.
- Boyd, K., Ebendorff-Heidepriem, H., Monroe, T. M., and Munch, J. (2012). Surface Tension and Viscosity Measurement of Optical Glasses Using a Scanning CO₂ Laser, *Optical Material Express*, 2(8), 1101-1110.

- Buerger, H., Vogel, W. and Kozhukarov, V. (1985). IR Transmission and Properties of Glasses in the $\text{TeO}_2 - \text{RnOm}$, RnXm , $\text{Rn}(\text{SO}_4)_m$, $\text{Rn}(\text{PO}_3)_m$ and B_2O_3 / System. *Infrared Physics*, 25, 395- 409.
- Cassie, A. B. D. and Baxter, S. (1944). Wettability of Porous Surfaces. *Transaction of the Faraday Society*, 40, 546-551.
- Cerne, L. and Simoncic, B. (2004). Influence of Repellent Finishing on the Surface Free Energy of Cellulosic Textile Substrates. *Textile Research Journal*, 74 (5), 426-432.
- Clearfield, A. (2008). *Introduction to Diffraction*. In John Wiley and Sons (Eds.) *Principles and Applications of Powder Diffraction* (73-121). Ltd Publications.
- Collet, B. M. (1972). A Review of Surface and Interfacial Adhesion in Wood Science and Related Fields. *Wood Science and Technology*, 6 (1), 1-42.
- Conti, G. N., Berneschi, S., Bettinelli, M., Brenchi, M., Chen, B., Pelli, S., Speghini, A., and Righini, G. C. (2004). Rare-Earth Doped Tungsten Tellurite Glasses and Waveguides: Fabrication and Characterization. *Journal of Non-Crystalline Solids*, 345, 343-348.
- Dousti, M. R., Sahar, M. R., Ghosal, S. K., Amjad, R. J. and Samavati, A. R. (2013). Effect of AgCl on Spectroscopic Properties of Erbium Doped Zinc Tellurite Glass. *Journal of Molecular Structure*, 1035, 6-12.
- Dousti, M. R., Amjad, R. J., Sahar, M. R., Zabidi, Z. M., Alias, A. N., and De Camargo, A. S. S. (2015). Er^{3+} - Doped Zinc- Tellurite Glasses Revisited : Concentration Dependent Chemical Durability, Thermal Stability and Spectroscopic Properties. *Journal of Non-Cryatalline Solids*, 429, 70-78.
- Durga, D. K. and Veeraiah, N. (2003). Role of Manganese Ions on the Stability of $\text{ZnF}_2 - \text{P}_2\text{O}_5 - \text{TeO}_2$ Glass System by the Study of Dielectric Dispersion and Some Other Physical Properties. *Journal of Physics and Chemistry of Solids*, 64, 133–146.

- El-Khoshkhany, N., Khatab, M. A., and Marva, A. K. (2018). Thermal, FTIR and UV Spectral Studies on Tellurite Glasses Doped with Cerium Oxide. *Ceramic International*, 44, 2789-2796.
- El-Mallawany, R. (1992). The Optical Properties of Tellurite Glass. *Journal of Applied Physics*, 72, 1774.
- El-Mallawany, R., El-Sayed, A. H., and El-Gawad, M. M. H. A. (1995). ESR and Electrical Conductivity Studies of (TeO₂) 0.95 (CeO₂) 0.05 Semiconducting Glasses. *Material Chemistry and Physics* 41(2), 87-91.
- El-Mallawany, R. (1998). Tellurite Glass Part 1. Elastic Properties. *Material Chemistry and Physics*, 53(2), 93-120.
- Eraiah, B. (2006). Optical Properties of Samarium Doped Zinc-Tellurite Glasses. *Bulletin of Material Science*, 29 (4), 375-378.
- Farouk, M., Samir, A., Metawe, F. and Elokr, M. (2013). Optical Absorption and Structural Studies of Bismuth Borate Glasses Containing Er³⁺ Ions. *Journal of Non-Crystalline Solids*, 371- 372, 14–21.
- Ghoshal, S. K., Asmahani, A., Sahar, M. R., and Arifin, R. (2015). Gold Nanoparticles Assisted Surface Enhanced Raman Scattering and Luminescence of Er³⁺ Doped Zinc-Sodium Tellurite Glass. *Journal of Luminescence*, 159, 265-273.
- Gindl, M., Sinn, G., Gindl, W., Reiterer, A. and Tschegg, S. (2001). A Comparison of Different Methods to Calculate the Surface Free Energy of Wood Using Contact Angle Measurements. *Colloids and Surfaces: A Physicochemical and Engineering Aspects*, 181 (1-3), 279-287.
- Goldstein, J. I., Newbury, D. E., Echlin, P., Joy, D. C., Fiori, C. and Lifshin, E. (1981). *Scanning Electron Microscopy and X-ray Microanalysis*. New York: Plenum Press.
- Henderson, G. S., and Wang, H. M. (2002). Germanium Coordination and the Germanate Anomaly. *Europe Journal Mineral*, 14, 733-744.

- Hirashima, H., Kurokawa, H., Mizobuchi, K., and Yoshida, T. (1988). Electrical Conductivity of Vanadium Phosphate Glasses Containing ZnO or GeO₂. *Glastechnische Berichte*, 61(6), 151-156.
- Hou, Z., Xue, Z., Wang, S., Hu, X., Lu, H., Niu, C., Wang, H., Wang, C., and Zhou, Y. (2012). Thermal Stability and Structure of Tellurite Glass. *Key Engineering Materials*, 512-515, 994-997.
- Johnson, P. A. V., Wright, A. C., Yarker, C. A. and Sinclair, R. N. J. (1986). A Neutron Diffraction Investigation of the Structure of Vitreous V₂O₅ – TeO₂. *Journal of Non-Crystalline Solids*, 81, 163-171.
- Kasap, S.O. (2006). *Principle of Electronic Materials and Devices*. (3rd ed.). New York: McGraw-Hill.
- Khandpur, R.S. (2007). *Handbook of Analytical Instruments*. New York: The McGraw- Hill Company, Inc.
- Kosuge, T., Benino, Y., Dimitrov, V., Sato, R. and Komatsu T. (1998). Thermal stability and Heat Capacity Changes at the Glass Transition in K₂O-WO₃-TeO₂ Glasses. *Journal of Non-Crystalline Solids*, 242, 154-164.
- Kozhukharov, V., Burger, H., Neov, S. and Sidzhimov, B. (1986). Atomic Arrangement of a Zinc-tellurite Glass. *Polyhedron*, 5, 771-777.
- Lafuma, A. and Quere, D. (2003). Superhydrophobic States. *Letter Nature Material. Journal of Applied Physics*, 2, 457.
- Lisi, D. and Licciuli, D. A. (2001/2002). Self-Cleaning Glass. *Scienza e Tecnologia dei Materiali Ceramici*, Corso di laurea in Ingegneria dei Materiali, Università Degli Studi Di Lecce.
- Martin, D.M. (2009). TeO₂ Based Film Glasses for Photonic Applications: Structural and Optical Properties. Laser Processing Group Universidad Investigaciones Cientcas Instituto de Optica Complutense de Madrid.

- Mohamed, N. B., Yahya, A. K., Deni, M. S. M., Mohamed, S. N., Halimah, M. K., and Sidek, H. A. A. (2010). Effects of Concurrent TeO₂ Reduction and ZnO Addition on Elastic and Structural Properties of (90-x)TeO₂-10Nb₂O₅-(x)ZnO Glass. *Journal of Non-Crystalline Solids*, 356, 1626-1630.
- Mohamed, E.A., Ahmad, F., and Aly, K. A. (2012). Effect of Lithium Addition on Thermal and Optical Properties of Zinc-Tellurite Glass. *Journal of Alloys and Compounds*, 538, 230-236.
- Murr, L.E., (1975). *Interfacial Phenomena in Metals and Alloys*. New York: Addison Wesley Publishing Co.
- Mazzola, L., Bemporad, E. and Carasiti, F. (2012). An Easy Way to Measure Surface Free Energy by Drop Shape Analysis. *Measurement*. 45 (3), 317-324.
- Nadargi, D. Y., Gurav, J. L., El Hawi, N., Rao, A. V., Koebel, M. (2010). Synthesis and Characterization of Transparent Hydrophobic Silica Thin Films by Single Step Sol- gel Process and Dip Coating. *Journal of Alloys Compound*, 496, 436-441.
- Nakajima, A., Hashimoto, K., and Watanabe, T. (2001). Recent Studies on Super Hydrophobic Films. *Chemical Monthly*. 132, 31-41.
- Nasu, H., Matsusita, O., Kamiya, K., Kobayashi, H., and Kubodera, K. (1990). Third Harmonic Generation from TeO₂ - Li₂O - TiO₂ Glasses. *Journal of Non-Crystalline Solids*. 124, 275-277.
- Nawaz, F., Sahar, M. R., Ghoshal, S. K., Asmahani, A., and Ishaq, A. (2014). Concentration Dependent Structural and Spectroscopic Properties of Sm³⁺/Yb³⁺ Co-doped Sodium Tellurite Glass. *Physica B*, 433, 89-95.
- Neumann, A. W. and Good, R.J. (1979). *Methods of Measuring Contact Angles*. In Good, R. J. and Stromberg, R. R. (Eds.) *Surface and Colloid Science* (31-91). New York: Plenum Press.
- Nurul Huda binti Abu Bakar (2012). *The Effect of Silylation Temperature on Silica Thin Films for Hydrophobic Studies*. Master of Science, Universiti Teknologi Malaysia, Skudai.

- Owens, D.K. and Wendt, R.C. (1969). Estimation of the Surface Free Energy of Polymers. *Journal of Applied Polymer Science*, 13 (8), 1741-1747.
- Özen, G., Demirata, B., Övec,og̃lu, M. L. and Genc, A. (2001). Thermal and Optical Properties of Tm³⁺ Doped Tellurite Glasses. *Spectrochimica Acta Part A*, 57, 273–280.
- Pantic´, M., Mitrovic´, S., Babic´, M., Jevremovic´, D., Kanjevac, T., Dzunic´, D., and Adamovic´, D. (2015). AFM Surface Roughness and Topography Analysis of Lithium Disilicate Glass Ceramic. *Tribology in Industry*, 37(4), 391-399.
- Pavani, P. G., Sadhana, K. and Mouli, V. C. (2011). Optical, physical and structural studies of boro-zinc tellurite glasses. *Physica B*, 406, 1242–1247.
- Pavia, D. L., Lampman, G. M., Kris, G. S. and Vyvyan, J. R. (2015). *Introduction to Spectroscopy*. (5th ed.). US: Cengage Learning.
- Pye, L. D. (1972). *The Vitreous State*. In Pye L.D., Stevens H. J. and LaCourse W.C. (Eds.) *Introduction to Glass Science* (1-30). US: Springer.
- Rajendran, V., Palanivelu, N., Chaudhuri, B. K., Goswami K. (2003). Characterization of Semiconducting V₂O₅ – Bi₂O₃ – TeO₂ Glasses Through Ultrasonic Measurements. *Journal of Non-Crystalline Solids*, 320, 195–209.
- Rajeswari, R., Surendra, S. B. and Jayasankar, C. K. (2010). Spectroscopic Characterization of Alkali Modified Zinc Tellurite Glasses Doped with Neodymium. *Spectrochimica Acta A*, 77 (1), 135-140.
- Rami Reddy, M., Ravi Kumar, V., Veeraiah, N., and Appa Rao, B. (1995). *Indian Journal of Pure and Applied Physics*, 33, 48.
- Redman, M., and Chen, J. (1967). Zinc Tellurite Glasses. *Journal of American Ceramic Society*, 50(10), 523-525.
- Rosmawati, S., Sidek, H. A. A., Zainal, A. T., and Mohd Zobir, H. (2007). IR and UV Spectral Studies of Zinc-Tellurite Glasses. *Journal of Applied Sciences*, 7 (20), 3051-3056.

- Sahar, M. R., and Noordin, N. (1995). Oxychloride Glasses Based on the $\text{TeO}_2 - \text{ZnO} - \text{ZnCl}$ System. *Journal of Non-Crystalline Solids*, 184, 137-140.
- Sahar, M. R., Jehbu, A. K. and Karim M. M. (1997). $\text{TeO}_2 - \text{ZnO} - \text{ZnCl}$ Glasses for IR Transmission. *Journal of Non-Crystalline Solids*, 213-214, 164-167.
- Sahar, M. R., Sulhadi, K., and Rohani, M. S. (2008). The Preparation and Structural Studies in the $(80-x)\text{TeO}_2 - 20\text{ZnO} - (x)\text{Er}_2\text{O}_3$ Glass System. *Journal of Non-Crystalline Solids*, 354, 1179-1181.
- Sanad, A. M., Moustafa, A. G., Moustafa, F. A., and El-Mongy, A. A. (1985). Role of Halogens on the Molar Volume of Some Glasses Containing Vanadium. *Central Glass and Ceramic Research Institute Bulletin*, 32(3), 53-56.
- Sara, M. Z., Alshimy, A. M. and Fahmy, A. E. (2014). Effect of Surface Treated Silicon Dioxide Nanoparticles on Some Mechanical Properties of Maxillofacial Silicon Elastomer. *International Journal of Biomaterials*, 2014, 1-4.
- Schrader, M. E. (1999). Work of Adhesion of a Sessile Drop to a Clean Surface. *Journal of Colloid and Interface Science*, 213, 602-605.
- Sekiya, T., Mochida, N. and Ohtsuka A. (1994). Raman Spectra of MO-TeO_2 (M = Mg, Sr, Ba and Zn) Glasses. *Journal of Non-Crystalline Solids*, 168, 106-114.
- Shelby, J. E. (2005). *Introduction to Glass Science and Technology*. The Royal Society of Chemistry, Cambridge, UK, 2nd Edition, 2005.
- Shimizugawa, Y., Maeseto, T., Inoue, S., Nukui A. (1997). Structure of $\text{TeO}_2\text{-ZnO}$ Glasses By Rdf And Te, Zn K Exafs, *Journal of Physical and Chemistry of Glasses*, 38 (4), 201-205.
- Sidebottom, D. L., Hruschka, M.A., Potter, B. G., and Brow, R. K. (1997). Structure and Optical Properties of Rare Earth-Doped Zinc Oxyhalide Tellurite Glasses – Practical Implications of Glass Structure. *Journal of Non-Crystalline Solids*, 222, 282-289.

- Sidek, H. A. A., Rosmawati, S., Talib, Z. A., Halimah, M. K., Daud, W. M. (2009). Synthesis and Optical Properties of ZnO – TeO₂ Glass System. *Journal of Applied Science*, 6, 1489-1494.
- Sidek, H. A. A., El-Mallawany, R., Siti, S. B., Halimah, M. K., and Khamirul, A. M. (2014). Optical Properties of Erbium Zinc Tellurite Glass System. *Hindawi, Advances in Material Sciences and Engineering*, 2015, 1-5.
- Sidkey, M. A., and Gaafar, M. S. (2004). Ultrasonic Studies on Network Structure of Ternary TeO₂ – WO₃ – K₂O Glass System. *Physica B: Condensed Matter*, 348, 46-55.
- Snoeijer, J. H. and Andreotti, B. (2008). A Microscope view on Contact Angle Selection, *Physics Fluids*, 20, 1-11.
- Sehlikeier, Y. H., Abdali, A., Hulser, T., Wiggers, H. and Schulz, C. (2012). Functionalization of SiO₂ Nanoparticles and Their Superhydrophobic Surface Coating. *NanoFormulation*, 113-120.
- Stanworth, J. E. (1950). *Physical Properties of Glass*. Oxford: Clarendon Press.
- Sulhadi, K. (2007). *Structural and Optical Properties Studies of Erbium Doped Tellurite Glass*. Ph.D Thesis, Universiti Teknologi Malaysia, Skudai.
- Surekha, K. and Sundararajan, S. (2015). *Self-Cleaning Glass*, In Aliofkhazraei M. (Auth.) *Anti-Abrasive Nanocoatings: Current and Future Applications* (81-103). Elsevier Ltd.
- Tanaba, S., Hirao, K., and Soga, N. (1990). Phonon Sideband of Eu³⁺ in Sodium Borate Glass. *Journal of Non-Crystalline Solids*, 122, 59-65.
- Tanko, Y. A., Sahar, M. R., and Ghoshal, S. K. (2016). Prominent Spectral Features of Sm³⁺ Ion in Disordered Zinc-Tellurite Glass. *Results in Physics*, 6, 7-11.
- Upendar, G., Vardhani, C. P., Suresh, S., Awasthi, A. M. and Mouli, V.C. (2010). Structure, Physical and Thermal Properties of WO₃ – GeO₂ – TeO₂ Glasses. *Materials Chemistry and Physics*, 121 (2010), 335-341.

- Van Uitert, L. G., and Wemple, S. H. (1978). ZnCl₂ glass: A Potential Ultra-Low Optical Fiber Material. *Applied Physics Letters*, 33, 57.
- Villegas, M. A. and Navarro, J. M. F. (2007). Physical and Structural Properties of Glasses in the TeO₂ – TiO₂ – Nb₂O₅ System. *Journal of European Ceramic Society*, 27 (7), 2715-2723.
- Wenzel, R.N. (1936). Resistance of Solid Surfaces to Wetting by Water. *Industrial Engineering Chemistry*, 28, 988-994.
- Widanarto, W., Sahar, M. R., Ghoshal, S. K., Arifin, R., Rohani, M. S., and Effendi, M. (2013). Thermal, Structural, Magnetic Properties of Zinc-Tellurite Glasses Cointaining Natural Ferrite Oxide. *Materials Letter*, 108, 289-292.
- Widanarto, W., Sahar, M. R., Ghoshal, S. K., Mashadi, Gustiono, D., and Effendi, M. (2014). Improved Thermal Features and Ionic Conductivity of Lithium-Zinc- Tellurite Glass Electrolytes. *Malaysian Journal of Fundamental and Applied Sciences*, 10(4), 207-2010.
- Wu, L., Bo, H., Yang, F., Qi, Y., Peng, S., Zhou, Y., and Li, J. (2015). Enhanced 1.53 μm Band Fluorescence in Er³⁺/ Ce³⁺ Codoped Tellurite Glasses Containing Ag NPs. *Optical Materials*, 43, 42-48.
- Yoneda, T. and Morimoto, T. (1999). Mechanical Durability of Water Repellent Glass. *Thin Solid Films*, 351, 279-283.
- Yuan, Y. and Lee T. R. (2013). *Contact Angle and Wetting Properties*. In Bracco, G. and Holst, B. (Eds.) *Surface Science Technique* (3-34). Springer.
- Yusof, N. N., Ghoshal, S. K., Arifin, R., Awang, A., Tewari, H. S., and Hamzah, K. (2018). Self-Cleaning and Spectral Attributes of Erbium Doped Sodium Zinc-Tellurite Glass : Role of Titania Nanoparticles. *Journal of Non-Cryatalline Solids*, 481, 225-238.
- Zamyatin, O. A., Churbanov, M. F., Medvedeva, J. A., Gavrin, S. A., and Zamyatina, E. V. (2018). Glass-Forming Region and Optical Properties of the TeO₂-ZnO-NiO System. *Journal of Non-Crytalline Solids*, 479, 29-41.

- Zenkiewicz, M. (2007). Methods for the Calculation of Surface Free Energy of Solids. *Journal of Achieve Manufacturing Engineering*, 24, 137-145.
- Zhang, Y., Lu, C., Feng, Y., Sun L., Ni, Y. and Xu Z. (2011). Effects of GeO₂ on the Thermal Stability and Optical Properties of Er³⁺/Yb³⁺-codoped Oxyfluoride tellurite glasses. *Journal of Material Chemistry Physics*, 126, 786–790.
- Zheng, S., Zhou, Y., Yin, D., Xu, X., Qi, Y., and Peng, S. (2013). The 1.53 μm Spectroscopic Properties and Thermal Stability in Er³⁺/ Ce³⁺ Codoped TeO₂-WO₃-Na₂O-Nb₂O₅ Glasses. *Journal of Quantitative Spectroscopy & Radiative Transfer*, 120, 44-51.

APPENDIX A

Pictures of Instruments Used

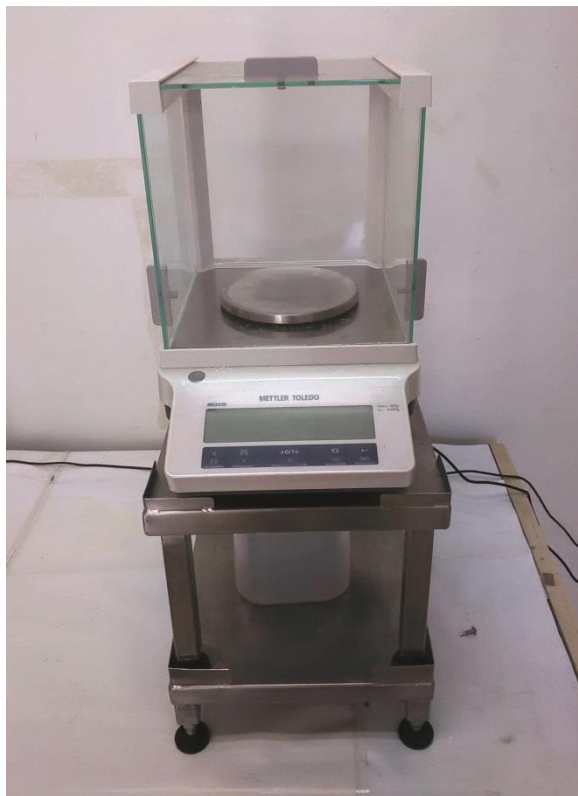


Figure A.1 : Density meter by Mettler Toledo available at Department of Physics, Faculty of Science, UTM.



Figure A.2 : Rigaku SmartLab X-ray diffractometer available at University Industry Research Laboratory, UTM.

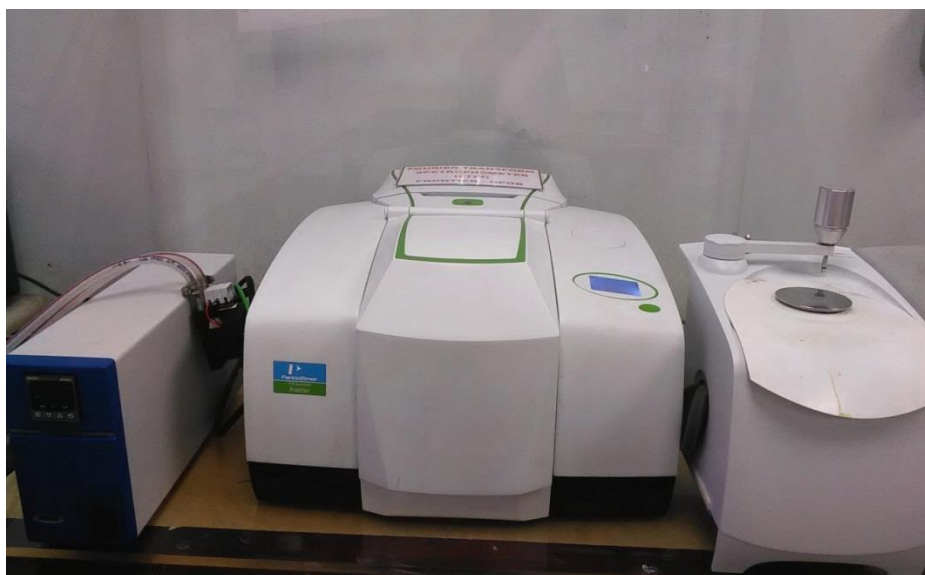


Figure A.3 : Perkin Elmer FTIR Spectrometer Frontier GPOB available at Chemistry Department, Faculty of Science, UTM.



Figure A.4 : Perkin Elmer STA 8000 available at University Industry Research Laboratory, UTM.

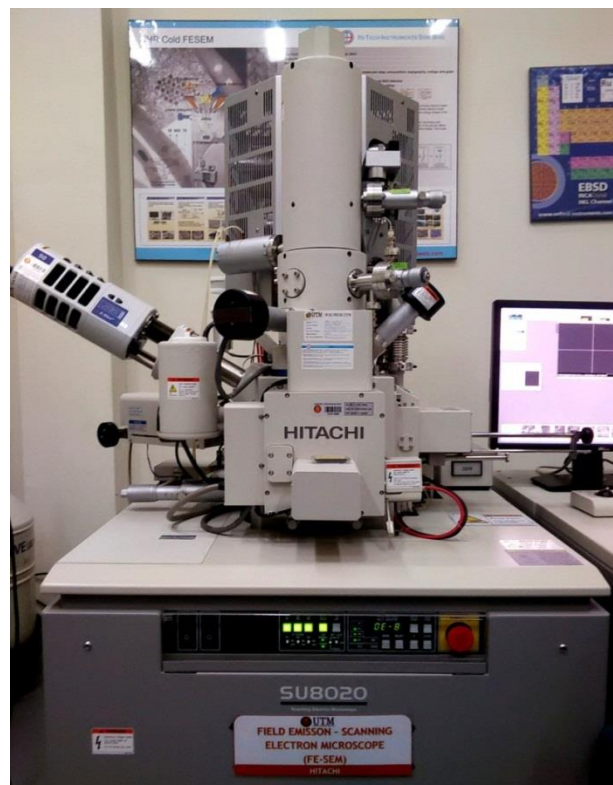


Figure A.5 : The hitachi SU8020 FESEM with EDX analysis available at University Industry Research Laboratory, UTM.



Figure A.6 : Atomic Force Microscope at Department of Physics, Faculty of Science, UTM.

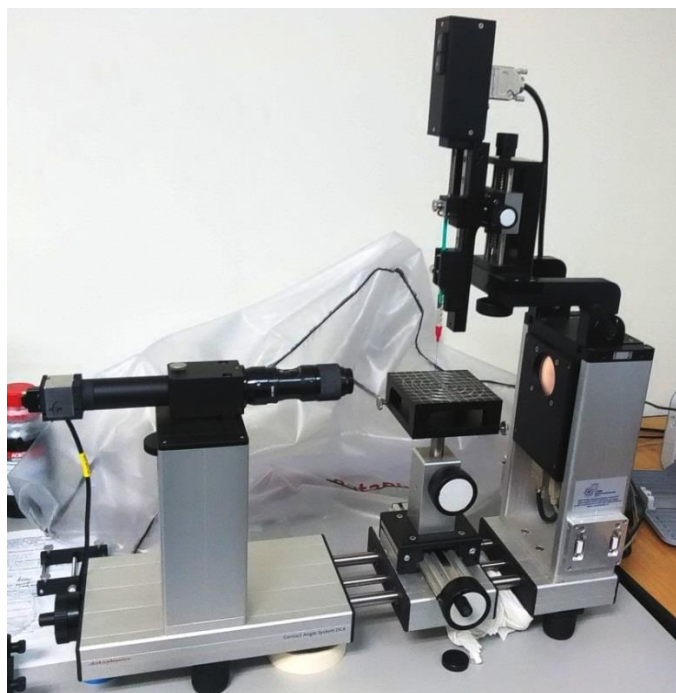


Figure A.7 : OCA meter by Data Physics available in Advance Membrane Technology Research Centre (AMTEC), UTM.

APPENDIX B

Calculation of Batch Sample Composition

Weight of sample = 15 g

Molar mass of each material:

- $\text{TeO}_2 = 159.5988 \text{ g/mol}$
- $\text{ZnO} = 81.3794 \text{ g/mol}$
- $\text{SiO}_2 = 60.0843 \text{ g/mol}$

Example of mass determination for glass composition of $(80-x) \text{ TeO}_2 - 20\text{ZnO} - (x) \text{ SiO}_2$ system ($x = 0.00, 0.05, 0.10, 0.15$ and 0.20)

SAMPLE 1

S1: $80\text{TeO}_2 - 20\text{ZnO}$

Total mol: $(0.80 \times 159.5988) + (0.20 \times 81.3794) = 143.9549 \text{ g/mol}$

For 15 grams batch of glass:

$$\text{TeO}_2 = \frac{(0.80 \times 159.5988)}{143.9549} \times 15 \text{ g} = 13.3041 \text{ g}$$

$$\text{ZnO} = \frac{(0.20 \times 81.3794)}{143.9549} \times 15 \text{ g} = 1.6959 \text{ g}$$

$$\begin{aligned} \# \text{ Total weight} &= 13.3041 + 1.6959 \\ &= 15 \text{ g.} \end{aligned}$$

SAMPLE 2

S2: 79.95 TeO₂ – 20ZnO – 0.05SiO

$$\begin{aligned} \text{Total mol: } & (0.7995 \times 159.5988) + (0.20 \times 81.3794) + (0.0005 \times 60.0843) = \\ & 143.9050 \text{ g/mol} \end{aligned}$$

For 15 grams batch of glass:

$$\text{TeO}_2 = \frac{(0.7995 \times 159.5988)}{143.9050} \times 15 \text{ g} = 13.3003 \text{ g}$$

$$\text{ZnO} = \frac{(0.20 \times 81.3794)}{143.9050} \times 15 \text{ g} = 1.6965 \text{ g}$$

$$\text{SiO}_2 = \frac{(0.0005 \times 60.0843)}{143.9050} \times 15 \text{ g} = 0.0031 \text{ g}$$

$$\begin{aligned} \# \text{ Total weight} &= 13.3003 + 1.6965 + 0.0031 \\ &= 15 \text{ g.} \end{aligned}$$

Calculation for other samples (S3, S4 and S5) are the same.

APPENDIX C**Calculation for Density of Sample**

$$\rho_s = \frac{w}{w-w'} \rho_o$$

where ρ_s is density of sample, w is weight in air, w' is weight in distilled water and ρ_o is density of distilled water.

Sample 1

Weight in air = 7.792 g

Weight in distilled water = 6.387 g

Density of distilled water = 1 g/cm³

$$\rho_{s1} = \frac{7.792}{(7.792-6.387)} (1) = 5.546 \text{ g/cm}^3$$

Calculation for other samples (S2, S3, S4 and S5) are the same.

Calculation for Uncertainty of Density

$$\Delta\rho_s = \left(\frac{\Delta w}{w} + \frac{\Delta(w-w')}{(w-w')} \right) \rho_s$$

Where $\Delta\rho_s$ is uncertainty of sample density while ρ_s is density of sample, w is weight in air, w' is weight in distilled water, uncertainty of weight in air, $\Delta w = 0.001$ and $\Delta(w-w') = 0.002$

Sample 1

$$\rho_{s1} = 5.546 \text{ g/mol}$$

$$w = 7.792 \text{ g}$$

$$w' = 6.387 \text{ g}$$

$$\Delta w = 0.001$$

$$\Delta(w-w') = 0.002$$

$$\Delta\rho_{s1} = \left(\frac{0.001}{7.792} + \frac{0.002}{1.405} \right) \times 5.546 = 0.009$$

Calculation for uncertainty of density for S2, S3, S4 and S5 are the same.

Calculation for Molar Volume of Sample

$$V_m = \frac{m}{\rho_s}$$

Where V_m is molar volume, ρ_s is density of sample and m is molecular weight.

Sample 1

Molecular weight for S1 = 143.9549 g/mol

Density of S1 = 5.546 g/cm³

$$V_m = \frac{143.9549}{5.546} = 25.957 \text{ cm}^3/\text{mol}$$

Calculation for other samples (S2, S3, S4 and S5) are the same.

Calculation for Uncertainty of Molar Volume

$$\Delta V_m = \left(\frac{\Delta m}{m} + \frac{\Delta \rho_s}{\rho_s} \right) V_m$$

Where ΔV_m is uncertainty of molar volume, V_m is molar volume of sample, $\Delta \rho_s$ is uncertainty of sample density while ρ_s is density of sample, $\Delta m = 0.001$ and m is molecular weight of sample

Sample 1

$\rho_{s1} = 5.546 \text{ g/mol}$

$$\Delta\rho_{s1} = 0.0086$$

$$\Delta m = 0.001$$

$$m = 143.9549 \text{ g/mol}$$

$$V_m = 25.957 \text{ cm}^3/\text{mol}$$

$$\Delta V_m = \left(\frac{0.001}{143.9549} + \frac{0.0086}{5.546} \right) \times 25.957 = 0.0404$$

Calculation for uncertainty of molar volume for S2, S3, S4 and S5 are the same.

APPENDIX D**Calculation for Surface Tension****Young-Dupre' Equation**

$$W_a = \gamma_L(1 + \cos \theta)$$

Sample 1

$$\gamma_L = 0.073 \text{ N/m}$$

$$\theta = 83.15^\circ$$

$$W_a = \gamma_L(1 + \cos \theta)$$

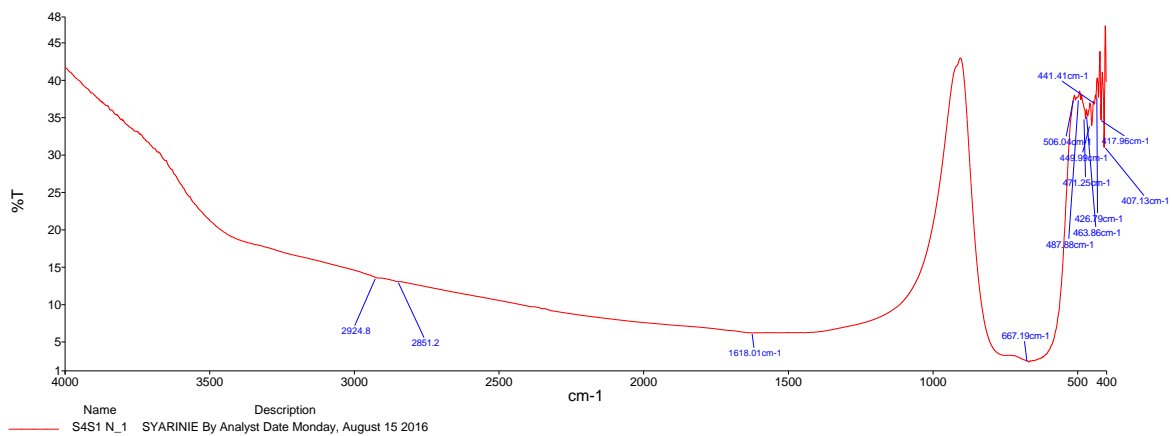
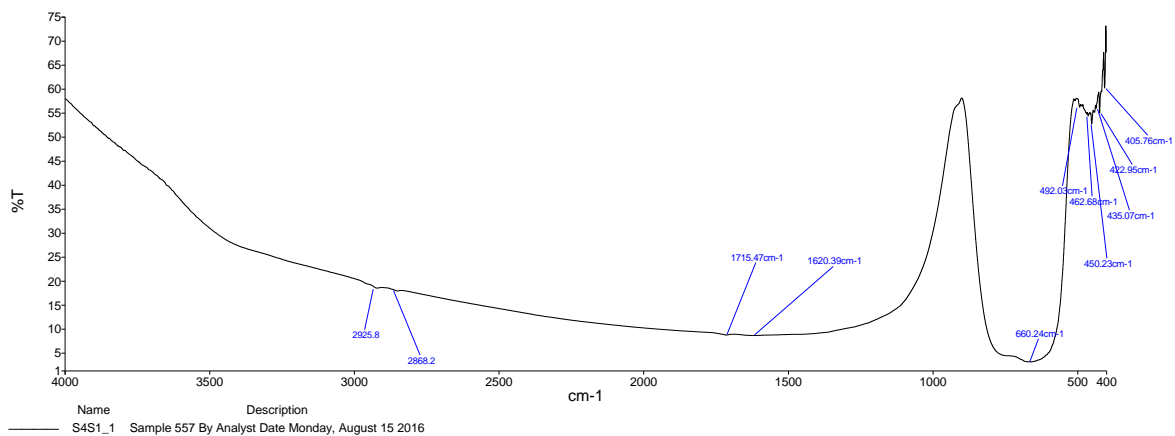
$$W_a = 0.073(1 + \cos 83.15)$$

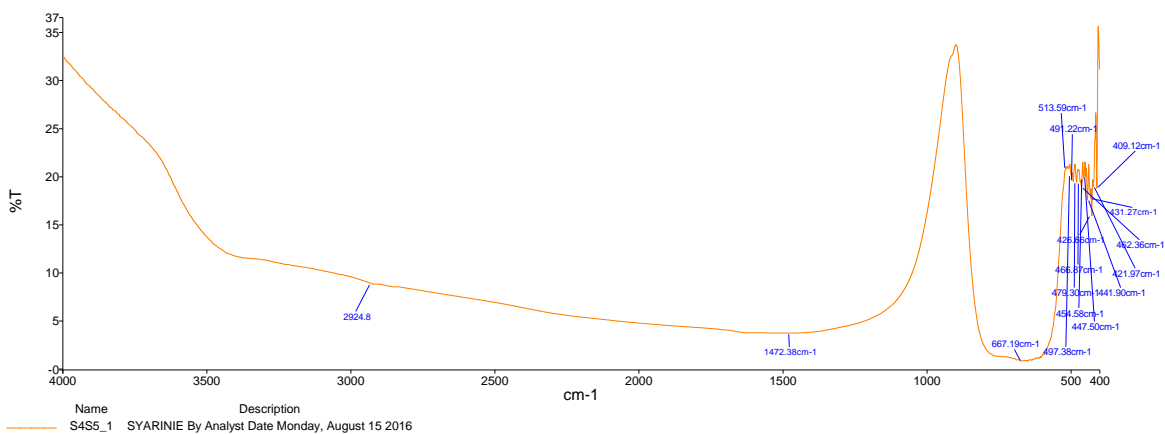
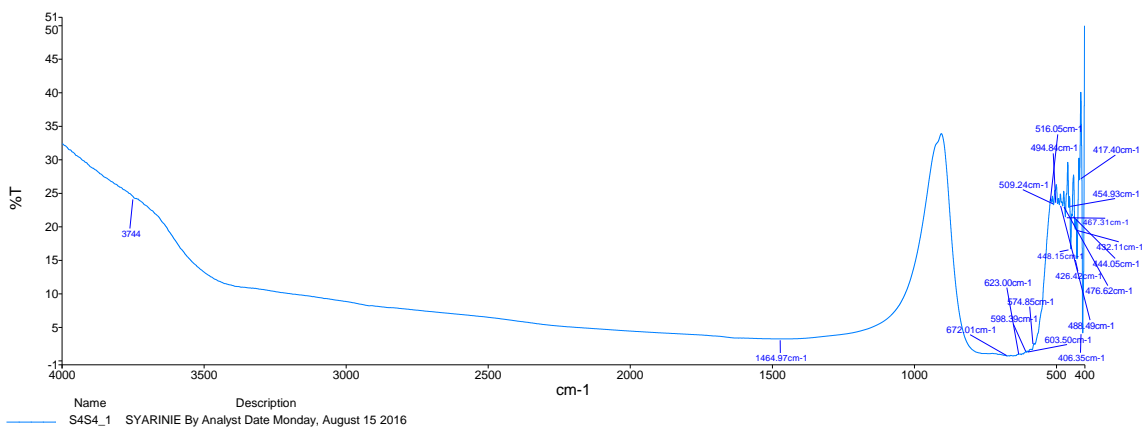
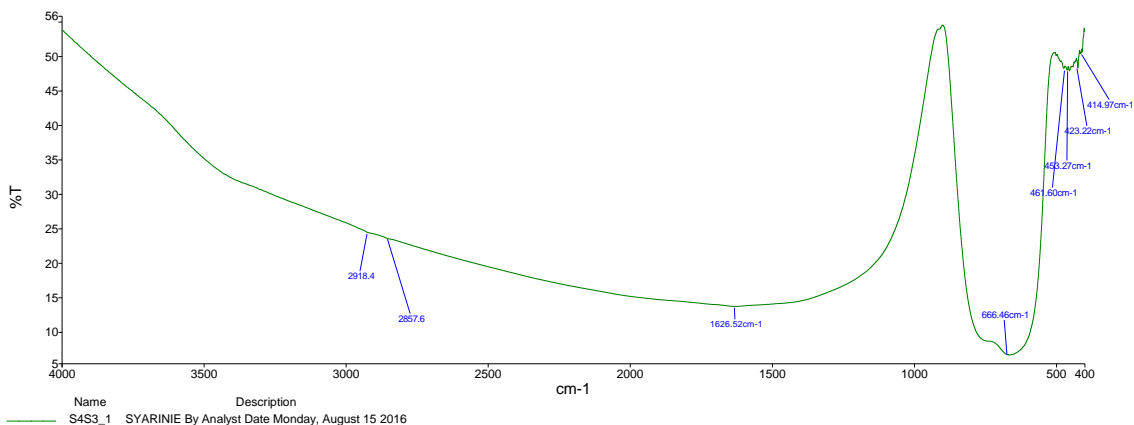
$$= 0.082 \text{ N/m}$$

Calculation for surface tension sample S2, S3, S4 and S5 are the same.

APPENDIX E

FTIR SPECTRA





APPENDIX F

List of Publications

Proceeding and Conference:

1. Azmi, S., Arifin, R. and Ghoshal, S. K. *Calcium Fluoride Concentration Effects on Thermal and Hydrophobic Properties of Zinc-Tellurite Glass*. 4th International Science Postgraduate Conference 2016 (ISPC 2016) at Ibnu Sina Institute, Universiti Teknologi Malaysia (UTM), Johor Bahru, Johor on 22-24 February 2016.
2. Azmi, S., Arifin, R. and Ghoshal, S. K. *Improved Hydrophobicity of Silicon Dioxide Integrated Zinc-Tellurite Glass Surface*. 29th Regional Conference on Solid State Science and Technology 2016 (RCSST 2016) at KSL Hotel, Johor Bahru, Johor on 15-17 November 2016.
3. Azmi, S., Arifin, R. and Ghoshal, S. K. (2017). Improved Hydrophobicity of Silicon Dioxide Integrated Zinc-Tellurite Glass Surface. *Solid State Phenomena*, 268, 87-91.